



The capability of Transmission Kikuchi Diffraction technique for characterizing nano-grained oxide scales formed on a FeCrAl stainless steel



N. Mortazavi^{a,*}, M. Esmaily^b, M. Halvarsson^a

^a Department of Applied Physics, Chalmers University of Technology, SE-412 96 Gothenburg, Sweden

^b Department of Chemical and Biological engineering, Chalmers University of Technology, SE-412 96 Gothenburg, Sweden

ARTICLE INFO

Article history:

Received 21 December 2014

Accepted 4 February 2015

Available online 11 February 2015

Keywords:

Metals and alloys

Oxidation

Microstructure

Nanocrystalline materials

Texture

ABSTRACT

This letter focuses on the capability of Transmission Kikuchi Diffraction (TKD) in Scanning Electron Microscope (SEM) for obtaining microstructural and micro-textural information from nano-grained oxide scales formed on a FeCrAl alloy. Orientation maps, with an indexing rate of 85%, showed the formation of grains in the range 20–300 nm. TKD revealed the existence of an orientation relationship at the alloy/oxide interface as well as the presence of a single grain (40 nm) with spinel structure in the alumina scale. A pre-tilted sample holder was designed for TKD investigations at short working distances with minimized mechanical drift of the thin foils.

© 2015 The Authors. Published by Elsevier B.V. This is an open access article under the CC BY-NC-ND license (<http://creativecommons.org/licenses/by-nc-nd/4.0/>).

1. Introduction

Often Transmission Electron Microscopy (TEM) is used to study the structure and chemical composition of nano-sized grains in the oxide scale formed on stainless steels. Conventional Electron Backscatter Diffraction (EBSD), which provides a spatial resolution of, at best, 20 nm [1], can also be used in Scanning Electron Microscope (SEM) to evaluate the oxide grain size distribution and to provide crystallographic information down to ~100 nm grain sizes [1]. For smaller grains, nano-diffraction techniques such as Convergent Beam Electron Diffraction (CBED) [2] in TEM are generally used in order to obtain crystallographic information with a spatial resolution of 2–5 nm [3–5]. However, as CBED pattern indexing is generally manual, it is not as fast as the EBSD technique, which uses automated indexing. Therefore, it is not possible to evaluate as many patterns by CBED as by EBSD.

Transmission Kikuchi Diffraction (TKD), also called transmission-Electron Backscatter Diffraction (t-EBSD) or transmission Electron Forward Scatter Diffraction (t-EFSD), is an electron diffraction method used in SEM that offers a dramatic improvement in spatial resolution over traditional EBSD. Since in the TKD analysis thin foils are used instead of bulk samples beam broadening is significantly reduced and accordingly the spatial resolution is decreased to 2–5 nm [7,6], which is comparable to nano-diffraction techniques in TEM. This method has recently been used to characterize metals with nano-sized grains

[6–11]. However, the research on the use of TKD method on microstructural characterization of oxide scale is in its very early stages. Fontaine et al. [12] have shown the benefit of simultaneous EDX and TKD to analyze the oxidation-assisted phase transformation in an austenitic stainless steel. TKD has also been applied for characterizing the microstructure of the oxide scale formed on a Zr-1.0%Nb zirconium alloy [13,14]. However, the authors in the later studies reported an indexing rate of ~40% in their TKD maps. This means that 60% of the data are missing and thus extracting some of the statistical data such as grain size distribution and grain boundary character is difficult and in some cases impossible. Therefore, the present study aims to show the capability of TKD in obtaining reliable microstructural and micro-textural information from nano-sized oxide scales developed on a FeCrAl alloy at high temperature.

2. Experimental

The microstructure of oxide scales formed on an alumina-forming FeCrAl alloy, with the commercial name of Kanthal APMT, was analyzed. Two different oxidizing environments were selected for this study; dry and wet atmosphere for 24 and 168 h at 1100 °C; see [15] for more details. An FEI Versa 3D combined Focused Ion Beam/Scanning Electron Microscope (FIB/SEM) workstation was used to produce thin foils. It was found that high-quality polished surface of the thin foils is of great importance for achieving to TKD maps with high indexing rate. Hence, lower accelerating voltages, i.e. 5 kV and 2 kV with ion current of 49 pA and 27 pA respectively, were used in

* Corresponding author. Tel.: +46 317723323.

E-mail address: nooshin.mortazavi@chalmers.se (N. Mortazavi).

the final thinning process. TKD analyses were performed using a HKL Channel 5 EBSD system with a Nordlys II detector, mounted on a Leo Ultra Field Emission Gun (FEG) SEM. An accelerating voltage of 30 kV in high current mode and an aperture size of 120 μm were used to maximize signal. The mapping was performed at a working distance (WD) of 3.5 mm, with a step size ranged from 5 to 10 nm, a tilting angle of 20° and a dwell time of about 0.18 s per pattern (s/pt). The total acquisition time was 1–4 h, depending on the area of analysis. The distance between the beam impact point on the specimen surface and the EBSD detector was about 15 mm. To further examine the TKD results of the oxidized samples, the foils were also investigated by Scanning Transmission Electron Microscopy (STEM) in a FEI Titan 80–300 TEM/STEM equipped with a FEG operated at an accelerating voltage of 300 kV. A High Angle Annular Dark Field (HAADF) detector was used to acquire STEM micrographs. Chemical compositional data were obtained using an Oxford Inca Energy Dispersive X-ray (EDX) detector. Quantitative data from EDX were obtained using standardless analysis.

3. Results and discussion

Performing high spatial resolution grain orientation mapping (in the nm range) of oxide scales is quite challenging. In order to collect high quality TKD patterns, it is of prime importance to optimize experimental parameters such as foil thickness and WD [10,16]. Another challenge in analyzing fine-grained oxides by the TKD is drift of the electron beam relative to the sample since the oxide scales are non-conductive. Additional problem is mechanical drift of the thin foil coming from drift of the SEM stage, thermal drift and/or sample contamination. Particularly at high magnification, which is the case for TKD investigations of small grains, mechanical stability of the thin foil sample mounting is important.

These essential needs for acquiring TKD maps with high indexing rates, called for designing a new sample holder for performing the TKD analyses on the oxide scales, see Fig. 1. This sample holder enables carrying out the TKD investigations at small WDs as the thin foil are positioned in the highest part of the holder. Moreover, it was noticed that the mechanical drift was decreased when using the new sample holder, which was exclusively designed for holding the thin foils for TKD analysis. This was probably linked to a better mechanical fixation of the thin foil by this holder. Furthermore, the holder gives the ability to insert a STEM detector in the SEM below the sample to capture STEM images from the same location as the TKD patterns and thereby achieving both imaging and crystallographic information. Using this holder, chemical compositional

analysis from the region of interest can also be done using EDX by lowering the stage to the analytical WD. In our experiment, the FIB-prepared thin foils were attached to copper grids. The brass holder in Fig. 1a shows the way of positioning the copper grid into the small thin foil holder that was later attached to the main sample holder, presented in Fig. 1b.

Fig. 2 shows a representative TKD analysis of the oxide layer of alloy APMT. The patterns were obtained with an average mean angular deviation (MAD) value of 0.4 and an indexing rate of 85%, signifying the excellent quality of the acquired data. The TKD maps show that the inner part of the oxide layer was composed of a large proportion of columnar grains in the range of 100–400 nm and a smaller number of nano-sized grains in the range of 40–100 nm. The outer part, however, was mainly composed of much smaller equiaxed grains in the range of 20–50 nm. Microstructural features are revealed in the band contrast map presented in Fig. 2b. It should be mentioned that band contrast is a quality factor calculated from the Hough transform (by the Oxford HKL Channel 5 software) and represent the overall quality of the diffraction patterns with values in the range 0–255 [17]. The black regions are more likely to be associated with pores, highly deformed grains or amorphous grains. The distribution of phases is seen in Fig. 2c. The structure of the oxide grains was corundum in both the inward and outward grown layers.

The orientation of grains can affect the oxidation behavior of metals [18–20]. The crystallographic orientation of the grains is shown in the inverse pole figure (IPF) colored map in Fig. 2d. The grain in the metal substrate had a near (101) orientation, while the grains of the oxide scale exhibited a strong $\langle 0001 \rangle$ texture with strength of 6.3 m.u.d. (multiples of uniform density), see Fig. 2e. The orientation relation between the crystals in the alumina scale and the grain in the metal substrate is schematically presented in Fig. 2d. The results show an orientation relationship $(110)_{\text{bcf}} // (0001)_{\text{corundum}}$ was present at the substrate/oxide scale interface, indicating that the planes of highest atomic density in the studied grains of the alumina scale and metal substrate were parallel. Such micro-textural studies can lead to a better understanding on the relationships between the orientation of grains in metal substrate and that of oxide scales.

Fig. 3 shows the SEM/TKD and STEM analyses of the oxide scale formed on the same alloy exposed in the wet environment. The STEM micrograph in Fig. 3b shows the inner and outer oxide scale layers as well as the presence of Reactive Element (RE) particles, rich in Yttrium (Y), in the alumina scale. Similar to the previous case, the TKD maps showed that the crystal structure of the grains in the inner and outer oxide layers was corundum (not shown). However, one small grain that was located in the outer oxide scale

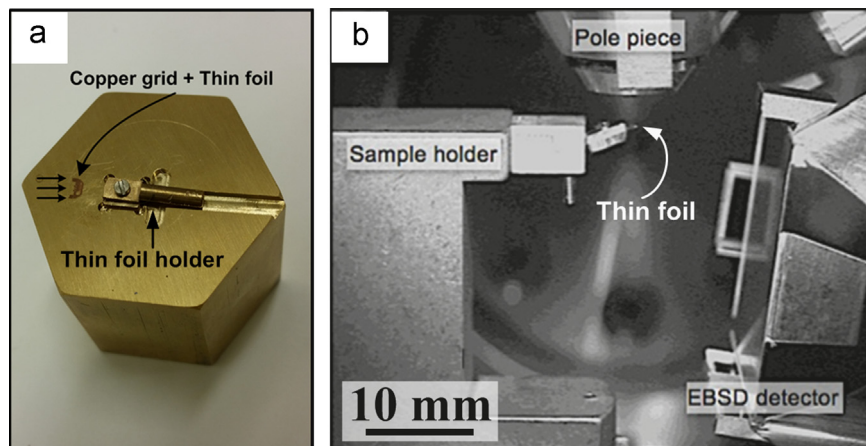


Fig. 1. (a) The brass holder designed for positioning the copper grid (containing the thin foil) into the sample holder, (b) In-chamber image of the newly designed TKD sample holder (made of aluminum) developed for the TKD experiments.

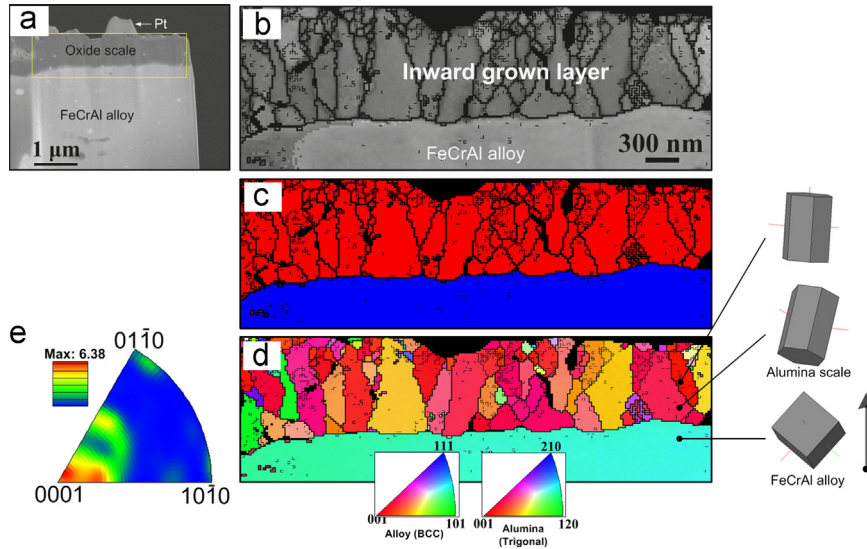


Fig. 2. (a) Secondary electron (SE) SEM image of the FIB-prepared cross section sample; the rectangle showing the region of TKD map. (b) TKD band contrast map showing the two-layered scale. (c) Phase map, the corundum structure of the oxide scale is designated by red, while the bcc alloy is blue. (d) Inverse Pole Figure (IPF) map with schematic drawings of some crystals. (e) IPF of the alumina scale, showing the strong $\langle 0001 \rangle$ -texture. (Alloy APMT exposed to the dry environment for 24 h at 1100 °C). (For interpretation of the references to color in this figure legend, the reader is referred to the web version of this article.)

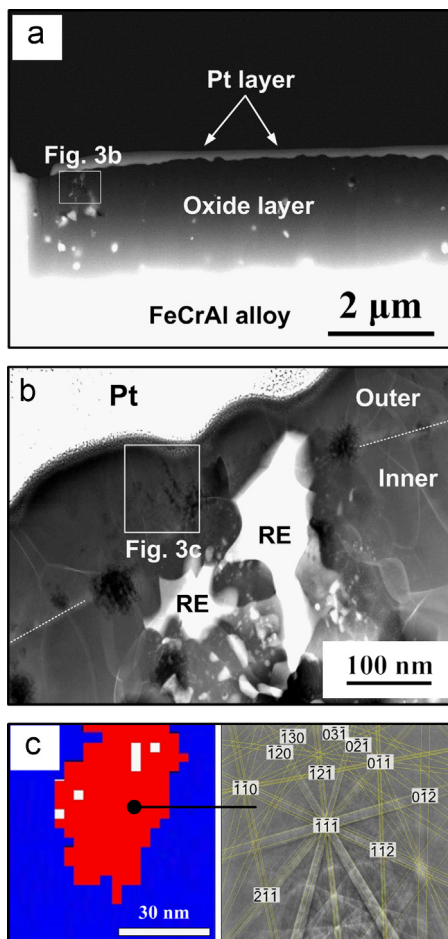


Fig. 3. (a) Overview SEM SE image of a FIB-prepared cross section sample. (b) STEM HAADF micrograph of the boxed area in Fig. 3a, (c) TKD phase map of the boxed area in Fig. 3b showing the detection of a single nano-sized grain (~ 40 nm) with spinel structure (shown by red) in a surrounding of grains with corundum structure (shown by blue) and the Kikuchi patterns of the grain with spinel structure. (Alloy APMT exposed to the wet environment for 168 h at 1100 °C). (For interpretation of the references to color in this figure legend, the reader is referred to the web version of this article.)

had a cubic (spinel-type) structure with the size of about 40 nm, as seen in the phase map in Fig. 3c. In order to explore the TKD result further, the same region was studied by STEM/EDX. It was revealed that the spinel grain contains 90 at% Al and 10 at% Fe (cationic), while the surrounding corundum structured grains contain less than 2 at% Fe. The presence of spinel grain (γ -alumina) in the oxide scale at such a high temperature and long exposure time of FeCrAl has not been reported previously [15,21]. It is suggested that the presence of Y in the vicinity alumina grain boundaries stabilizes the spinel structure; see [22] for more details. Identifying this grain is of technological importance, as it is known that γ -alumina, which has a spinel structure, causes a loss in protectiveness properties of the oxide scale and thus deteriorates the oxidation resistance of the alloy [23]. This type of nano-scale phase identification of a large number of grains, which makes it possible to identify one single spinel grain surrounded by many grains with corundum structure, shows the strength of the TKD technique for studying nano-sized oxide scales, which is also simple, fast and reliable compared to the TEM based techniques.

4. Conclusions

In summary, we have reported the use of TKD technique as a promising high-resolution analytical technique for performing advanced microstructure characterization on nano-sized oxide scales developed on the alumina-forming alloys at high temperatures. Grain orientation mapping with high indexing rate was obtained using this SEM-based method, which is inexpensive, automated and fast, compared to other high-resolution nanodiffraction methods. Using optimized acquisition parameters and a new dedicated sample holder crystallographic information from grains as small as 20 nm was reliably obtained. The TKD was effectively employed for phase identification and texture analysis of the nano-grained oxide scale formed on a FeCrAl alloy.

References

- [1] Schwarzer R, Field DP, Adams BL, Kumar M, Schwartz AJ. *Electron Backscatter Diffraction in Materials Science*. New York: Springer; 2009.

- [2] Williams DB, Carter CB. *Transmission Electron Microscopy - A Textbook for Materials Science*. New York: Springer; 2009.
- [3] Zaefferer S. *Crystal Res Tech* 2011;47:607–28.
- [4] Wu G, Zaefferer S. *Ultramicroscopy* 2009;109:1317–25.
- [5] Liu HH, Schmitd S, Poulsen HF, Godfrey A, Liu ZQ, Sharon JA, et al. *Science* 2011;332:833–4.
- [6] Brodusch N, Demers H, Gauvin R. *J Microsc* 2013;250:26–32.
- [7] Trimby PW. *Ultramicroscopy* 2012;120:16–24.
- [8] Keller RR, Geiss RH. *J Microsc* 2012;245:245–51.
- [9] Sha G, Tugcu K, Liao XZ, Trimby PW, Murashkin MY, Valiev RZ, Ringer SP. *Acta Mater* 2014;63:169–79.
- [10] Suzuki S. *JOM* 2013;65:1254–63.
- [11] Trimby PW, Cao Y, Chen Z, Han S, Hemker KJ, Lian J, et al. *Acta Mater* 2014;62:69–80.
- [12] Fontaine AL, Yen HW, Trimby P, Moody S, Miller S, Chensee M, et al. *Corros Sci* 2014;85:1–6.
- [13] Garner A, Gholinia A, Frankel P, Gass M, MacLaren I, Preuss M. *Acta Mater* 2014;80:159–71.
- [14] Hu J, Garner A, Ni N, Gholinia A, Nicholls RJ, Lozano-Perez S, et al. *Micron* 2015;69:35–42.
- [15] Hellström K, Israelsson N, Mortazavi N, Canovic S, Halvarsson M, Svensson JE, et al. *Oxid Met* 2015;83:1–26.
- [16] Brodusch N, Demers H, Trudeau M, Gauvin R. *Scanning* 2013;35:375–86.
- [17] Zhou A, Wang ZL. *Scanning Microscopy for Nanotechnology: Techniques and Applications*. New York: Springer; 2006.
- [18] Tolpygo VK, Clarke DR. *Acta Mater* 1998;14:5153–66.
- [19] Jonsson T, Pujilaksono B, Hallström S, Ågren J, Svensson JE, Johansson LG, et al. *Corros Sci* 2009;51:1914–24.
- [20] Kim BK, Szpunar JA. *Scr Mater*. 2001;44:2605–10.
- [21] Golightly FA, Stott FH, Wood GC. *Oxid Met* 1976;10:163–87.
- [22] Götlind H, Liu F, Svensson JE, Halvarsson M, Johansson LG. *Oxid Met* 2007;67:251–66.
- [23] Segerdahl K, Svensson JE, Johansson LG. *Mater Corros* 2002;53:247–55.